Automatic Detections of Nipple and Pectoralis Major in Mammographic Images

Yi-Chong Zeng

***Abstract*--After diagnosing, doctors record diagnostic results as structure data. For example, they record mass position by referring to relative positions of another object not coordinate. Those objects include tissues of breast and areas of human body. This paper presents schemes to detect nipple and pectoralis major. For nipple detection, we consider cases of visible and invisible nipples. Our scheme computes curvature of edge between breast and background, and then finds convex area or largest curvature, which is considered as nipple. In mediolateral oblique (MLO) view image, edge appears between pectoralis major and non-muscle. For pectoralis major detection, the proposed scheme applies Smith-Waterman algorithm to scoring matrix referred to MLO image. Finally, boundary of pectoralis major is defined as path with minimum score. The experiment results demonstrate that the proposed scheme has good performances in nipple and pectoralis major detections.**

I. INTRODUCTION

Mammography is a common way for lesion diagnosis of breast. Doctors analyze mammographic image and then find suspected regions. After diagnosing, doctors record diagnostic results as structure data. For example, they record mass position by referring to relative positions of another object not coordinate. Those objects include tissues of breast and areas of human body. There were literatures addressed how to detect objects in mammography. Jas et al. [1] estimated farthest pixel from base which is either edge of pectoral muscle in mediolateral oblique (MLO) view mammography or vertical axis in craniocaudal (CC) view mammography. Nipple position is defined as the farthest pixel. In [2], Chae et al. developed algorithms for considerations of visible and invisible nipple detections. For invisible nipple detection, they targeted to analyze location of fibroglandular tissue instead of nipple.

For pectoralis major detection, Kwok et al. [3] implemented iterative threshold selection for estimating straight line in region of interest. They further utilized iterative cliff detection to refine estimated lines fit to boundary of pectoral muscle. In [4], Cardoso et al. detected pectoral muscle contour based on shortest path. They transformed image into polar domain, and then searched path between the top and the bottom rows. In [5], Mustra and Grgic combined adaptive histogram equalization and polynomial curvature estimation for edge detection as well as pectoral muscle detection. Chuang performed optical density transformation on MLO image to generate contrast-transformed image [6, 7]. Subsequently, he utilized Canny detection to detect pectoral muscle in contrast-transformed image.

In this paper, we propose schemes to detect nipple and pectoralis major on MLO images. Both cases of visible and invisible nipples are analyzed in this work. The proposed scheme computes curvature of edge between breast and background. Then, nipple is defined as convex area or a point with largest curvature. For pectoralis major detection, Smith-Waterman algorithm is implemented on scoring matrix that is generated based on MLO image. Consequently, our scheme searches path with minimum score which is treated as boundary of pectoralis major. Cardoso et al.'s approach [4] and ours utilizes path searching in pectoralis major detection. However, our scheme has lower computation complexity than [4]. The rest of this paper is organized as follows: problem statement is described in Section II. The proposed nipple and pectoralis major detections are introduced in Sections III and IV, respectively. The experiment results will be revealed in Section V, and the conclusion will be drawn in Section VI.

This study is conducted under the "Advanced Artificial Intelligence Technologies and Industry Applications Project (1/4)" of the Institute for Information Industry which is subsidized by the Ministry of Economic Affairs of the Republic of China.

II. PROBLEM STATEMENT

Mammographic image consists of multiple objects, such as, nipple, pectoralis major, fibrous tissue, fatty tissue, and mammary glands. Those objects are helpful for doctors recording diagnostic results as structured data. For example, Fig.1 shows that mass is marked by a red circle in the MLO images. In the right side of figure, structured data reveal the 1st detected mass locates at anterior third of lower inner quadrant. Doctors can easily find the mass based on professional knowledge in medical; however, it is a challenge to machine to render data as well as detect mass. Rendering the above description, the anterior third of lower inner quadrant means that the lesion locates at the bottom one-third of distance between nipple and axilla. The axilla is identified as the bottom of boundary of pectoralis major. Therefore, object plays an important role for rendering structured data.

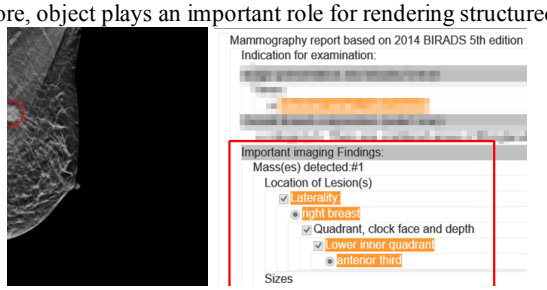

Fig.1. Mammographic image (left) and structured data (right)

III. NIPPLE DETECTION

Chae et al. [2] developed nipple detection by considering visible and visible nipples. Visible nipple always bulges on boundary of breast and background is around it. As nipple locates within area of breast, it is named invisible nipple. Fig.2(a) show two cases of nipple appearances.

A. Visible Nipple Detection

The first procedure is to extract background. Due to intensity of background is always lower than that of foreground. Therefore, our scheme utilizes thresholding approach to separate background I_G and foreground (breast) I_B. As the (x,y)-th pixel value is smaller than or equal to the threshold α, the pixel is considered as a part of background and $I_G(x,y)=1$. Subsequently, closing of morphological operation is applied to I_G to yield the filtered background I_F. The differences between I_G and I_F is computed and clustered pixels into several areas. Finally, nipple is defined as the largest area adjacent to breast.

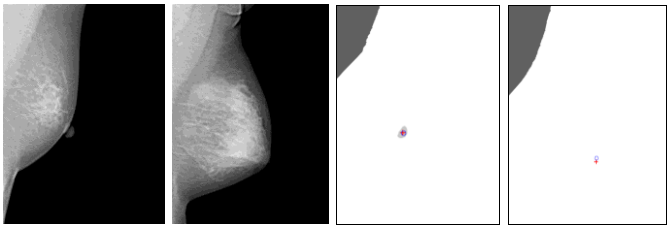

(a) (b)

Fig.2. Nipple Appearances and Detection Results: (a) visible nipple (left) and invisible nipple (right), and (b) detected results of (a)

B. *Invisible Nipple Detection*

According to architecture of breast in mammography, nipple locates at high curvature of edge. The proposed method finds edge between area of breast and background in advance. Then, curvatures of pixels on the half-length middle edge are computed. Let (x_i, y_i) be coordinate of the i-th pixel on the half-length middle edge. Curvature referred to [8] is formulated below,

$$c_i = \frac{x_i' y_i'' - y_i' x_i''}{\left(x'^2 + y'^2\right)^{\frac{3}{2}}} \tag{1}$$

where c_i represents curvature of the i-th pixel. The denotations Z'_i and Z''_i are, respectively, first-order differential and second-order differential of Z-axis sequence of the i-th pixel, and $Z \in \{x, y\}$. Finally, the coordinate (x_j, y_j) of c_j with largest curvature is estimated by,

$$j = \underset{i \in \{1,2,\cdots,N\}}{arg\ max}(c_i) \tag{2}$$

where the denotation N is the total number of pixels on the middle edge. In this case, nipple position is defined as (x_j, y_j).

IV. PECTORALIS MAJOR DETECTION

In Fig.2(a), the light-gray areas at the top-left corners of image are pectoralis majors. An edge obviously appears between pectoralis major and non-muscle. Our scheme detects edge as well as pectoralis major. First, right MLO image is flipped horizontally, and left MLO image is unchanged. Therefore, breast always locates at the left of image. Subsequently, Unsharp masking [9] and median filter are applies to MLO image to result filtered-binary image I_{MF}. Analyzing MLO image, edge starts at top row and ends at left column. We refer to local sequence alignment to search path as well as detect edge using Smith-Waterman algorithm. Let $M(x,y)$ be the accumulated score at (x,y)-th pixel of scoring matrix, and scoring matrix is computed by,

$$M(x,y) = \begin{cases} I_{MF}(x,y) & \text{if } y = 1 \text{ and } I_B(x,y) = 1 \\ \underset{k \in \{-1,0,1\}}{\text{argmin}}\left(M(x+k, y-1)\right) + I_{MF}(x,y) & \text{if } 1 < y \le H \text{ and } I_B(x,y) = 1 \\ \infty & \text{otherwise} \end{cases} \tag{3}$$

where H denotes height of image. Meanwhile, our scheme records the linkage of the current pixel to the previous one. During path searching, the initial starting pixel is at first column of scoring matrix, which has minimum accumulated score. According to linkages of pixels, the process finds the previous pixel and sets it as next starting pixel. Finally, the path is yielded by collecting all pixels, and it is treated as edge between pectoralis major and non-muscle. Finally, pectoralis major is defined as the encircled area by the detected edge, the first row and the first column of image.

V. THE EXPERIMENT RESULTS

A. *Nipple Detection*

Twenty MLO images were tested in the first experiment. The two tested images are shown in Fig.2(a). The areas of detected nipples are shown in Fig.2(b) illustrated by light-gray areas. Moreover, red cross and blue circle are, respectively, the centers of detected nipple and ground truth. For performance evaluation of nipple detection, rate of coordinate difference was computed by,

$$r_X = \frac{1}{W}\left|x_{GT} - x_{EXP}\right| \times 100\%, \text{and } r_Y = \frac{1}{H}\left|y_{GT} - y_{EXP}\right| \times 100\%, \tag{4}$$

where Z_{GT} and Z_{EXP} represent the Z-axis coordinates of ground truth and experiment result, respectively, and , and $Z \in \{x,y\}$. In the experiment, the average rates of coordinate differences to x-axis and y-axis were, respectively, r_X=2.29% and r_Y=1.86%.

B. *Pectoralis Major Detection*

Fig.2(b) shows detected pectoralis majors of Fig.2(a), which are illustrated as the dark-gray areas at the top-left corner of image. Four quantitative measures were computed for evaluation of pectoralis major detection, including, precision, recall, accuracy, and F-measure. TABLE I lists the average measures of the 20 images tested using [7] and ours. Our scheme had good performance in pectoralis major detection, and all measures are above 0.96.

VI. CONCLUSION

This paper presents schemes to detect nipple and pectoralis major in mediolateral oblique view images automatically. For nipple detection, our scheme is capable of dealing with both visible nipple and invisible nipple. The experiment results demonstrate the average rates of coordinate differences between ground truth and detected result are r_X=2.29% and r_Y=1.86%. For pectoralis major detection, the proposed scheme has higher accuracy than the existing approach. All of the four measures are above 0.96 averagely.

TABLE I
AVERAGE MEASURES OF THE EXISTING APPROACH [7] AND OUR SCHEME

Measures	Chuang's approach [7]	Our Scheme
Precision	**0.998**	0.968
Recall	0.53	**0.97**
Accuracy	0.87	**0.98**
F-measure	0.65	**0.97**

REFERENCES

[1] M. Jas, S. Mukhopadhyay, J. Chakraborty, A. Sadhu, N. Khandelwal, "A heuristic approach to automated nipple detection in digital mammograms," *Journal of Digital Imaging*, vol.26, no.5, pp.932-940, Oct. 2013.

[2] S.-H. Chae, J.-W. Jeong, J.-H. Choi, E. Y. Chae, H. H. Kim, Y. –W. Choi, and S. Lee, "Fully automated nipple detection in digital breast tomosynthesis," *Computer Methods and Programs in Biomedicine*, vol.143, no.C, pp.113-120, May 2017.

[3] S. M. Kwok, R. Chandrasekhar, Y. Attikiouzel, M. T. Rickard, "Automatic pectoral muscle segmentation on mediolateral oblique view mammograms," *IEEE Trans. Medical Imaging*, vol.23, no.9, pp.1129-1140, Sept. 2004.

[4] J. S. Cardoso, I. Domingues, I. Amaral, I. Moreira, P. Passarinho, J. S. Comba, R. Correia, M. J. Cardoso, "Pectoral muscle detection in mammograms based on polar coordinates and the shortest path," *32nd Annual International Conference of the IEEE in Engineering in Medicine and Biology Society* (*EMBC*), pp.4781-4784, Aug. 31 – Sept. 4, 2010.

[5] M. Mustra, M. Grgic, "Robust automatic breast and pectoral muscle segmentation from scanned mammograms," *Signal Processing*, vol. 93, no.10, pp.2817–2827, 2013.

[6] M. Sameti, R. K. Ward, J. Morgan-Parkes, B. Palcic, "Image feature extraction in the last screening mammograms prior to detection of breast cancer," *IEEE Journal of Selected Topics in Signal Processing*, vol.3, no.1, pp.46-52, Feb. 2009.

[7] C.-J. Chuang, "Mammographics mass detection by different sized windows in optical density images," Master Thesis, National Cheng Kung University, June 2013.

[8] Y.-C. Zeng, "Decomposition and construction of object based on law of closure in gestalt psychology," *IEEE Global Conf. on Consumer Electronics* (*GCCE*), pp.770-773, Oct. 2017.

[9] Unsharp masking, [online] https://en.wikipedia.org/wiki/Unsharp_masking